Palmitate-Induced Vacuolar-Type H(+)-ATPase Inhibition Feeds Forward Into Insulin Resistance and Contractile Dysfunction

Palmitate-Induced Vacuolar-Type H^+-ATPase Inhibition Feeds Forward Into Insulin Resistance and Contractile Dysfunction

Yilin Liu,[1] Laura K.M. Steinbusch,[1] Miranda Nabben,[1] Dimitris Kapsokalyvas,[2] Marc van Zandvoort,[2] Patrick Schönleitner,[3] Gudrun Antoons,[3] Peter J. Simons,[4] Will A. Coumans,[1] Amber Geomini,[1] Dipanjan Chanda,[1] Jan F.C. Glatz,[1] Dietbert Neumann,[1] and Joost J.F.P. Luiken[1]

Diabetes 2017;66:1521–1534 | https://doi.org/10.2337/db16-0727

Dietary fat overconsumption leads to myocardial lipid accumulation through mechanisms that are incompletely resolved. Previously, we identified increased translocation of the fatty acid transporter CD36 from its endosomal storage compartment to the sarcolemma as the primary mechanism of excessive myocellular lipid import. Here, we show that increased CD36 translocation is caused by alkalinization of endosomes resulting from inhibition of proton pumping activity of vacuolar-type H^+-ATPase (v-ATPase). Endosomal alkalinization was observed in hearts from rats fed a lard-based high-fat diet and in rodent and human cardiomyocytes upon palmitate overexposure, and appeared as an early lipid-induced event preceding the onset of insulin resistance. Either genetic or pharmacological inhibition of v-ATPase in cardiomyocytes exposed to low palmitate concentrations reduced insulin sensitivity and cardiomyocyte contractility, which was rescued by CD36 silencing. The mechanism of palmitate-induced v-ATPase inhibition involved its dissociation into two parts: the cytosolic V_1 and the integral membrane V_0 subcomplex. Interestingly, oleate also inhibits v-ATPase function, yielding triacylglycerol accumulation but not insulin resistance. In conclusion, lipid oversupply increases CD36-mediated lipid uptake that directly impairs v-ATPase function. This feeds forward to enhanced CD36 translocation and further increased lipid uptake. In the case of palmitate, its accelerated uptake ultimately precipitates into cardiac insulin resistance and contractile dysfunction.

Overconsumption of lipids is associated with high risks of developing heart failure (1,2). The heart exposed to high lipid concentrations displays elevated rates of long-chain fatty acid (LCFA) uptake, which often exceeds the capacity of the mitochondria to oxidize the LCFA so that lipids accumulate inside the cardiomyocytes (3,4). Lipid oversupply induces mitochondrial dysfunction over time, thereby aggravating the mismatch between LCFA uptake and oxidation (3,5). Lipid oversupply in combination with other factors, such as high sucrose consumption, may ultimately lead to contractile dysfunction (5). Importantly, the mechanisms of chronically elevated LCFA uptake involve altered dynamics of LCFA transporters (3).

Whereas the heart expresses four membrane LCFA transporters (CD36, FABPpm, FATP1, and FATP4), studies with CD36-null animals demonstrate that ~70% of cardiac LCFA uptake is mediated via CD36 (3). In the heart, CD36 is not only present at the sarcolemma but is also stored in intracellular membrane compartments (endosomes), from where it can translocate to the sarcolemma to increase LCFA uptake (3). Insulin is the main hormonal stimulus to induce CD36 translocation, leading to increased LCFA uptake for subsequent storage into triacylglycerols (3,6). Insulin-induced CD36 translocation closely resembles the well-characterized insulin-induced GLUT4 translocation from endosomes to the cell surface to increase cardiac glucose uptake (3). Hence, CD36 translocation is a key regulatory mechanism of cardiac LCFA uptake.

[1]Department of Molecular Genetics, CARIM School for Cardiovascular Diseases, Maastricht University, Maastricht, the Netherlands
[2]Department of Molecular Cell Biology, CARIM School for Cardiovascular Diseases, Maastricht University, Maastricht, the Netherlands
[3]Department of Physiology, CARIM School for Cardiovascular Diseases, Maastricht University, Maastricht, the Netherlands
[4]Bioceros BV, Utrecht, the Netherlands

Corresponding author: Joost J.F.P. Luiken, j.luiken@maastrichtuniversity.nl.

Received 10 June 2016 and accepted 13 March 2017.

This article contains Supplementary Data online at http://diabetes.diabetesjournals.org/lookup/suppl/doi:10.2337/db16-0727/-/DC1.

D.N. and J.J.F.P.L. are co-senior authors.

In insulin-resistant rodent models, CD36 has been found responsible for the chronically elevated LCFA influx upon lipid overload (7,8). Concordantly, CD36-null mice are protected against the development of lipid-induced cardiomyopathy (9,10). CD36 protein expression does not change during cardiac lipid overload. Rather, the net translocation of CD36 from endosomes to the sarcolemma is increased, indicating that lipid oversupply induces chronic changes in subcellular CD36 cycling. In rodent models of lipid-induced cardiomyopathy, the chronically elevated uptake of LCFA into cardiomyocytes is coupled to accumulation of triacylglycerol within lipid droplets and formation of diacylglycerols/ceramides (7,8). These lipid metabolites impair insulin signaling at the level of insulin receptor substrate 1/2 or Akt2 (11), which then leads to inhibition of insulin-stimulated GLUT4 translocation and glucose uptake (3,8). Insulin resistance, therefore, would be expected to also impair insulin-stimulated CD36 translocation and LCFA uptake. However, CD36-dependent lipid uptake is highly upregulated in the insulin-resistant heart. Hence, how increased CD36 translocation evolves from lipid oversupply remained elusive.

We previously obtained evidence that endosomal alkalinization causes a rapid translocation of CD36, but not of GLUT4, to the sarcolemma (12). By active import of protons, vacuolar-type H^+-ATPase (v-ATPase) acidifies the lumen of vesicular organelles, among which are endosomes. The multimeric v-ATPase protein complex consists of 14 subunits: 6 subunits form the integral membrane subcomplex V_0, encompassing the proton channel, and 8 subunits make up a peripheral membrane subcomplex V_1, containing the ATP-binding pocket (13–15).

In this study, we first analyzed v-ATPase function in cardiomyocytes in vivo and in vitro during chronic lipid oversupply. Secondly, we made a detailed assessment in time of the onset of v-ATPase inhibition compared with increased LCFA uptake and insulin resistance. Thirdly, we studied whether genetic or pharmacological inhibition of v-ATPase affects insulin resistance and contractile dysfunction and clarified the involvement of CD36. Fourthly, we investigated functional alterations of v-ATPase in human stem cell–derived cardiomyocytes subjected to excess lipids. Finally, we determined the mechanism and LCFA specificity of v-ATPase inhibition.

RESEARCH DESIGN AND METHODS

The experiments in this study were performed according to Dutch regulations and approved by the Maastricht University Committee for Animal Welfare.

Experimental Animals and Isolation and Culturing of Primary Rat Cardiomyocytes

Male Lewis rats (200–250 g) were purchased from Charles River Laboratories and fed a 10% low-fat diet (D12450B; Research Diets, New Brunswick, NJ) or a 60% high-fat diet (D12492). After 7 weeks of the diet, cardiomyocytes were isolated as previously described (16). For the in vitro studies, rats were fed standard chow before the isolation of cardiomyocytes. Then, culturing was performed for ≤48 h in low-palmitate and high-palmitate media as previously described (17). For selected experiments, cultured primary cardiomyocytes were treated with oleate replacing palmitate at the same concentrations or with blocking antibodies against CD36 (clone 63, Bioceros BV) as previously described (17). Extensive control experiments using this antibody for CD36 blockade were published previously (17).

Cell Culture of HL-1 Cardiomyocytes and Transfection

HL-1 cells were cultured in control medium as previously described (18). We also used low-palmitate and high-palmitate media containing 100 nmol/L insulin and 500 nmol/L or 20 μmol/L palmitate, respectively, complexed to 3.3 μmol/L BSA, resulting in palmitate-to-albumin ratios of 0.15:1 (low palmitate) and 6:1 (high palmitate). When indicated, oleate was used instead of palmitate at the same concentrations. At 24 h after seeding, cells were transfected at 60–70% confluence using 10 pmol small interfering (si) RNA and 2 μL Lipofectamine RNAiMAX per well in antibiotic- and noradrenaline-free culture medium. After 6 h, medium was refreshed with growth medium, and 48 h after transfection cell lysis or functional assays were performed. In preparation of testing short-term insulin action, media were removed and replaced by control medium. At 30 min thereafter, insulin (or an equal volume of H_2O) was added for another 30 min before the measurements, as described below.

Human Induced Pluripotent Stem Cells Differentiated Into Cardiomyocytes

Human induced pluripotent stem cells (iPSCs) were provided by Dr. F. van Tienen (Maastricht University Medical Center) and differentiated into cardiomyocytes (iPSC-CMs) according to the manufacturer's protocol (Thermo Fisher Scientific). All treatments on iPSC-CMs were performed as indicated for HL-1 cardiomyocytes.

CD36 Cell Surface Staining

Two-photon microscopy to visualize cell surface CD36 localization and colorimetric CD36 detection at the sarcolemma using a horseradish peroxidase–linked secondary antibody were performed as previously described (17,19).

Measurement of Substrate Uptake

[1-^{14}C]palmitate and [1-^{3}H]deoxyglucose uptake into suspensions of primary cardiomyocytes was measured as previously described (6). Uptake of these substrates into HL-1 cardiomyocytes and into cultured primary cardiomyocytes, with both cell models seeded on precoated glass slides, was measured as previously described (17,18).

Measurement of Triacylglycerol Content

Myocellular triacylglycerol accumulation was measured as previously described (19).

Measurement of Cellular Chloroquine Accumulation as Readout of v-ATPase Function

Chloroquine accumulation was measured as previously described (12).

Microscopical Imaging of Endosomal Acidification

Primary cardiomyocytes were cultured for 1.5 h in adhesion medium and then incubated for 15 min with 500 nmol/L LysoSensor DND-189 for subsequent imaging with a Leica TCS SP5 (Leica Microsystems GmbH, Wetzlar, Germany) two-photon microscope. Then, 100 nmol/L bafilomycin-A was added, and a second image was captured. Excitation was at 820 nm, and a Leica objective HCX APO L ×20/1.00 was used for excitation and epi-collection. LysoSensor Green (DND-189, Invitrogen) fluorescence signal was detected at 470–550 nm.

Measurement of Cardiomyocytic Contraction Dynamics

Contractile properties of cardiomyocytes were assessed at 1 Hz field stimulation using a video-based cell geometry system to measure sarcomere dynamics (IonOptix). From the digitized recordings, contractile parameters (sarcomere shortening, time to peak, and decay time) were calculated as previously described (17).

Measurement of Colocalization of v-ATPase and CD36

Cardiomyocyte suspensions were subjected to subcellular fractionation as previously described (6), yielding a low-density microsomal fraction enriched in endosomes. Aliquots (100 μg) were incubated with anti-IgG, anti-CD36, or anti–v-ATPase a2 antibodies overnight at 4°C in the absence of detergents. Then, the antibody-captured low-density microsomal vesicles were coupled to protein-A Sepharose-4 beads for 4 h at 4°C. Further preparation of the vesicles for analysis of coimmunoprecipitation was performed as earlier described (18).

Measurement of v-ATPase Disassembly

Two methods were applied for analysis of disassembly.

1. Immunoprecipitation: HL-1 cardiomyocytes were washed twice with ice-cold PBS and lysed with lysis buffer containing 1% Brij O20, 250 mmol/L NaCl, 5 mmol/L EDTA, and 50 mmol/L HEPES (pH 7.0). A 500 μg cell suspension was incubated overnight at 4°C with control IgG or specific antibodies recognizing v-ATPase B2 or a2 subunits. The protein-antibody complex was coupled to Sepharose-4 beads for 4 h at 4°C. Beads were washed five times in lysis buffer, boiled in sample buffer, and centrifuged, after which the supernatant was used for Western blotting.
2. Fractionation: HL-1 cardiomyocytes were fractionated into membrane and cytoplasmic fractions, as previously described (20), for further analysis by Western blotting.

Cell Lysis and Western Blotting

Cell lysis and Western blotting were performed as described earlier (6). Antibody details are provided in the Supplementary Data online. The signals were normalized to caveolin-3 (loading control). Then, a second normalization was performed by setting the control incubation (low-fat diet, control, or low-palmitate condition, depending on the experiment) at 1.

mRNA Expression of Cardiac-Specific Genes

Total RNA was isolated as previously described (10), and quantitative real-time PCR was performed using SYBR Green (Bio-Rad) and the following primer sequences (5′→3′): CTCCGTGAAGGGATAACCAGG (MYH6-F), GGGCCTCTAG ACGCTCCTT (MYH6-R), AGCGGAAAAGTGGGAAGAGG (TNNT2-F), CACAGCTCCTTGGCCTTCTC (TNNT2-R), CAC GAACCACGGCACTGATT (TBP-F), and TTTTCTTGCTGCCA GTCTGGAC (TBP-R). Samples were normalized using TBP as a housekeeping gene.

Statistics

All data are presented as mean ± SEM. Statistical analysis was performed by using two-sided Student *t* test, and we applied paired testing when possible. *P* values of <0.05 were considered statistically significant.

RESULTS

In the Rodent Heart, CD36 Colocalizes With v-ATPase on Endosomes

Rat cardiomyocytes were fractionated for the purification of the endosome-containing low-density microsomal fraction. As anticipated, v-ATPase subunits a2 (as part of the cytosolic V_0 subcomplex) and B2 (as part of the integral membrane V_1 subcomplex) were both more prominently present in the microsomal fraction compared with the total cardiomyocyte lysate (Fig. 1*A*). This fraction was subsequently used for immunoprecipitation in the absence of detergents (i.e., to keep the vesicular membranes intact). Upon immunoprecipitation using CD36-directed antibodies, all of the a2 subunit and most of the B2 subunit was found in the pellet fraction, whereas no a2 and few B2 were found in the supernatant fraction (Fig. 1*A*). In a reverse immunoprecipitation, using antibodies against a2, CD36 was almost completely captured as well as most of B2 (Fig. 1*A*). Hence, under basal conditions, the majority of CD36 and v-ATPase colocate to the same endosomal vesicles.

Lipotoxic Conditions Decrease v-ATPase Function in Cardiomyocytes In Vivo and In Vitro

Lewis rats were fed a low-fat diet (10% fat) or a high-fat diet (60% fat) for 7 weeks. As expected, body weight and heart mass were significantly increased in the group fed the high-fat diet (Supplementary Fig. 1*A* and *B*), whereas blood glucose levels remained in the normal range (Supplementary Fig. 1*C*). Upon subcellular fractionation, cardiomyocytes from rats fed the high-fat diet displayed increased localization of CD36 at the plasma membrane and decreased content in the low-density microsomal fraction (that includes endosomes). GLUT4 localization showed the opposite response: increased low-density microsomal and decreased plasma membrane abundance (Supplementary Fig. 1*D*). Hence, in the high-fat diet condition, CD36 preferentially translocated to the sarcolemma, whereas GLUT4 internalized

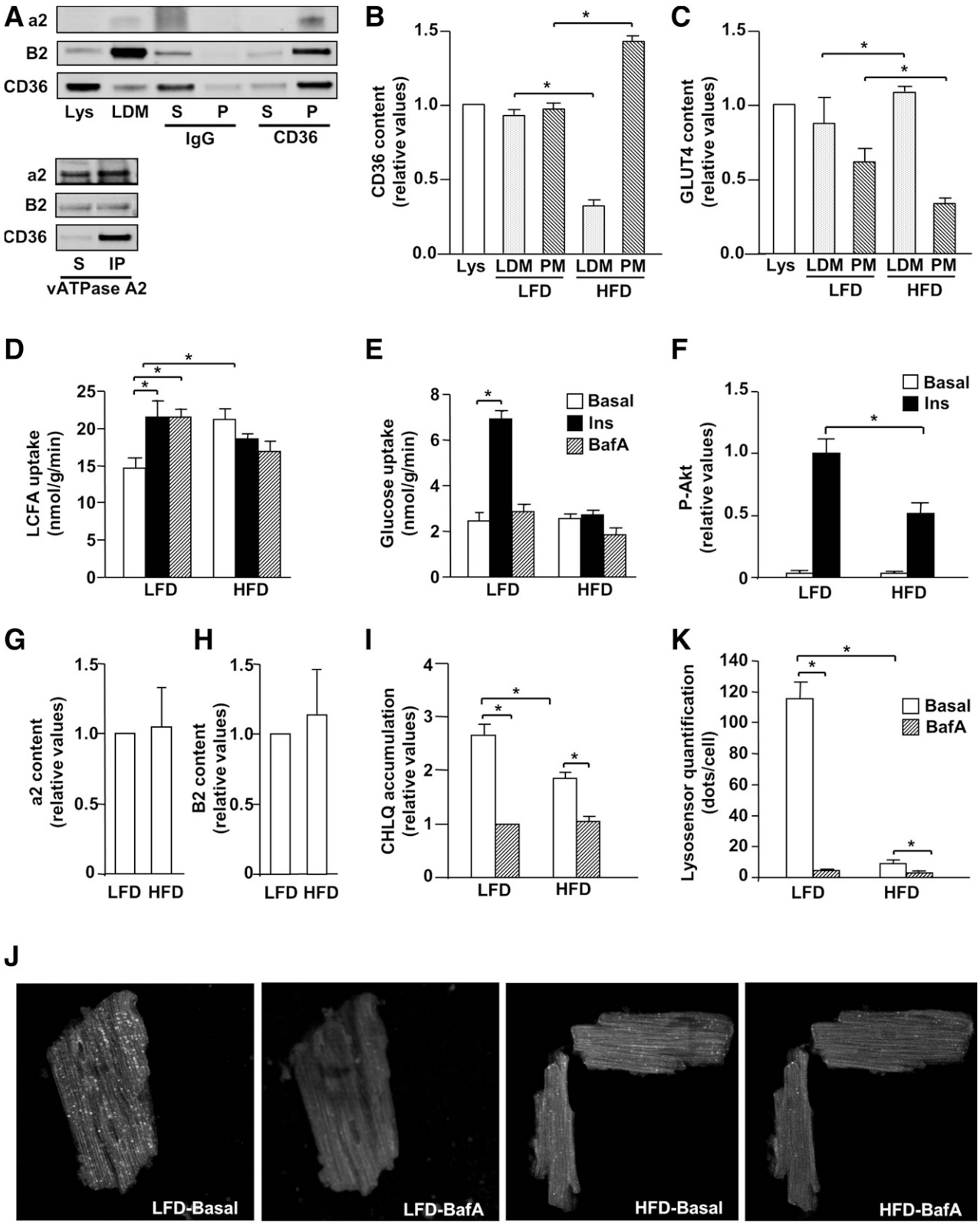

Figure 1—High-fat diet impairs v-ATPase function in cardiomyocytes. *A*: Immunoprecipitation (IP) of CD36 or v-ATPase subunit a2 or IgG control from low-density microsomal (LDM) fractions (enriched in endosomes) prepared from primary rat cardiomyocytes. IP samples were immunoblotted with antibodies against CD36 and v-ATPase subunits a2 and B2. Lys, cardiomyocyte lysates; P, pellet of IP; S, supernatant of IP. Immunoblots are representative results ($n = 3$). *B–K*: Cardiomyocytes were isolated from Lewis rats after being fed a low-fat diet (LFD) or high-fat diet (HFD) for 7 weeks. *B* and *C*: CD36 and GLUT4 presence in cell lysate (Lys), at the plasma membrane fraction (PM), and in the LDM fraction after subcellular fractionation ($n = 3$). *D* and *E*: LCFA and glucose uptake into cardiomyocytes treated without/with insulin (Ins) or bafilomycin-A (BafA) for 15 min (LFD: $n = 6$; HFD: $n = 10$). *F*: Akt phosphorylation (P-Akt) after treatment of cardiomyocyte suspensions

to the microsomal fraction (Fig. 1*B* and *C*). Increased CD36 translocation to the sarcolemma was associated with increased basal LCFA uptake (Fig. 1*D*). Furthermore, short-term (20-min) insulin treatment stimulated LCFA and glucose uptake into cardiomyocytes in the low-fat diet but not the high-fat diet condition (Fig. 1*D* and *E*). Insulin-induced Akt phosphorylation was also disturbed in the high-fat diet condition (Supplementary Fig. 1*E*; quantification in Fig. 1*F*).

Focusing on v-ATPase, the protein expression levels of the V_0 subunit a2 and V_1 subunit B2 were unaffected by the diet (Fig. 1*G* and *H*). As a readout of v-ATPase function, we measured cellular accumulation of the divalent weak base chloroquine, which becomes specifically trapped in acidic organelles (21). For calibration of this assay, we used bafilomycin-A, a potent v-ATPase inhibitor (20-min incubation). The bafilomycin-A–sensitive component of the total cellular chloroquine accumulation reflects v-ATPase activity. In low fat–diet cardiomyocytes, the bafilomycin-A–sensitive component presents 62% of cellular chloroquine accumulation (Fig. 1*I*). Whereas the bafilomycin-A–insensitive component was unaltered in high fat–diet cardiomyocytes, the bafilomycin-A–sensitive component was decreased by 52%, thereby indicating a halfway inhibition of v-ATPase upon lipid overload. v-ATPase function was also assessed with the fluorescent pH indicator LysoSensor DND-189 in combination with two-photon microscopy. Application of LysoSensor to low fat–diet cardiomyocytes yielded a particulate staining pattern (gray dots, Fig. 1*J*). Subsequent incubation with bafilomycin-A resulted in a nearly complete disappearance of the dots within <20 min, suggesting that LysoSensor specifically visualizes organelles that are acidified by v-ATPase. Importantly, the number of dots per cell in comparison with the low-fat condition was much lower in high fat–diet cardiomyocytes (Fig. 1*K*). Taken together, the biochemical and microscopic methods both indicate that v-ATPase function is inhibited in the lipid-overloaded heart.

To investigate a possible causal link between v-ATPase inhibition and increased CD36-mediated LCFA uptake, cardiomyocytes from low- and high fat–diet rats were incubated with bafilomycin-A (20 min) before substrate uptake assays. Bafilomycin-A caused LCFA uptake to increase to a similar level as insulin treatment of low fat–diet cardiomyocytes, whereas no significant effect of the inhibitor was observed in high fat–diet cardiomyocytes (Fig. 1*C*). Hence, the mechanism of increased basal LCFA uptake in high fat–diet cardiomyocytes might include v-ATPase inhibition. Short-term treatment with bafilomycin-A did not alter glucose uptake (Fig. 1*C*). Therefore, CD36 trafficking is regulated by v-ATPase function, whereas GLUT4 is not.

The main LCFA species of the lard-based high-fat diet, which was used for the described animal studies, is palmitate. Thus, we next investigated the palmitate-induced changes in v-ATPase activity in cultured cardiomyocytes. After 48 h, the high-palmitate culturing condition induced an elevation in surface CD36 content without changing CD36 total expression, indicating increased CD36 translocation to the sarcolemma (Fig. 2*A* and *B*). Accordingly, LCFA uptake (Fig. 2*C*) and triacylglycerol content (Fig. 2*F*) were increased upon high-palmitate treatment, whereas insulin-stimulated LCFA/glucose uptake and Akt phosphorylation were decreased and contractile function was impaired (Fig. 2*C–E* and *G*). Moreover, we observed a 60% decrease in v-ATPase function in cardiomyocytes treated with high palmitate versus low palmitate (bafilomycin-A–sensitive chloroquine accumulation) (Fig. 2*H*). Similar results were seen in mouse-derived HL-1 cardiomyocytes upon lipid oversupply (Supplementary Fig. 2). Hence, cellular palmitate oversupply decreases v-ATPase function and leads to insulin resistance and contractile dysfunction.

Palmitate Oversupply Causes v-ATPase Inhibition Before the Onset of Insulin Resistance

Primary cardiomyocytes were exposed to variable periods of high-palmitate culturing. We assessed v-ATPase function (by chloroquine accumulation) as well as LCFA/glucose uptake and Akt/S6 phosphorylation in the absence/presence of insulin. From the chloroquine data (Fig. 3*A*), the bafilomycin-A–sensitive component was deduced as readout of v-ATPase activity (Supplementary Fig. 3*A*). The insulin-sensitive component was similarly calculated for substrate uptake and Akt/S6 phosphorylation status (Supplementary Fig. 3*B–E*). Under low-palmitate culturing conditions, endosomal pH, substrate uptake, and insulin sensitivity did not change (Fig. 3*A–E* and Supplementary Fig. 3*A–E)*. In contrast, high-palmitate culturing induced a rapid 34% decrease in v-ATPase function within the first hour, which was followed by a slower rate of decline (Fig. 3*A*). In addition, basal LCFA uptake increased by 1.5-fold within the first hour, with no further increase thereafter (Fig. 3*B*). This rapid increase in basal LCFA uptake was accompanied by a rapid loss of insulin-sensitive LCFA uptake (Fig. 3*B* and Supplementary Fig. 3*B*). Reductions in insulin-sensitive glucose uptake

without/with 100 nmol/L Ins (LFD: $n = 4$; HFD: $n = 4$). *G* and *H*: Protein expression of v-ATPase subunit a2 or B2 in cardiomyocytes (LFD: $n = 4$; HFD: $n = 4$). *I*: Chloroquine (CHLQ) accumulation in cardiomyocytes treated without/with BafA for 15 min (LFD: $n = 5$; HFD: $n = 6$). *J*: LysoSensor imaging in cardiomyocytes from LFD and HFD rats treated without BafA (basal) and with BafA for 15 min. Representative microscopic images are displayed for each condition. *K*: Quantification is expressed as the number of dots per cell (LFD: $n = 6$; HFD: $n = 6$; 5 cells were analyzed from each cardiomyocyte preparation). Values are displayed as mean ± SEM. *$P < 0.05$. Data were normalized to Lys (*B* and *C*), LFD/basal (*F*), LFD (*G* and *H*), or to LFD/BafA (*I* and *K*).

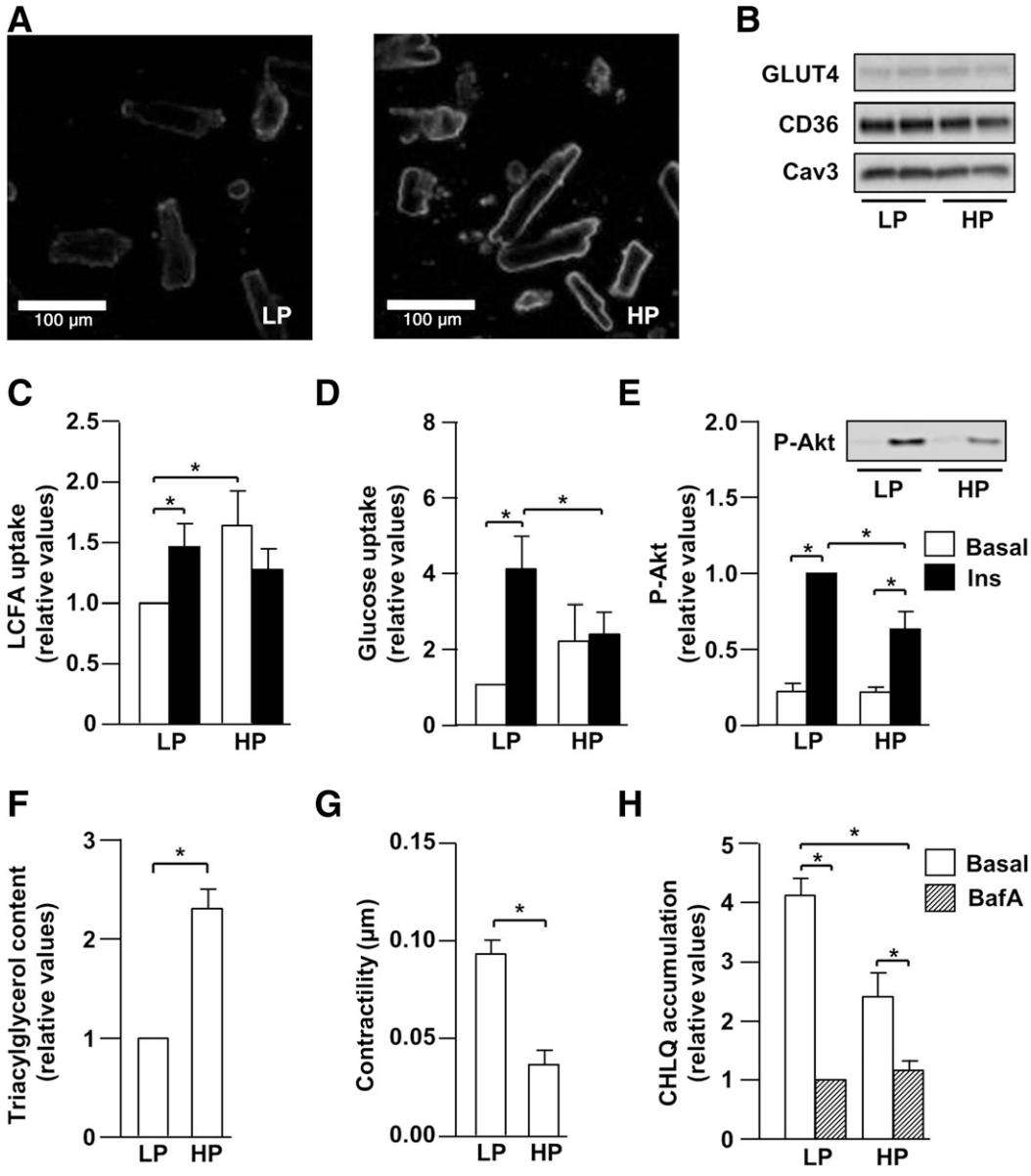

Figure 2—Lipid overload induces v-ATPase inhibition in cultured cardiomyocytes. Rat cardiomyocytes were cultured for 48 h in media containing low palmitate (LP) and high palmitate (HP). *A*: Cell surface abundance of CD36 protein using two-photon microscopy (n = 3; representative images are shown). *B*: Protein expression of GLUT4 and CD36. Caveolin-3 (Cav3) was the loading control (n = 3). *C–E*: LCFA and glucose uptake (n = 5) and Akt phosphorylation (P-Akt; n = 5) in cardiomyocytes treated without (basal)/with 100 nmol/L insulin (Ins) for 15 min. A representative blot is shown. *F–H*: Triacylglycerol content (n = 5), sarcomeric shortening at 1 Hz field stimulation (n = 5; imaging of 3 cells/condition), and chloroquine (CHLQ) accumulation in cardiomyocytes treated without (basal)/with 100 nmol/L bafilomycin-A (BafA) for 15 min (n = 5). Values are displayed as mean ± SEM. *P < 0.05. Data were normalized to LP/basal (*C* and *D*), LP/Ins (*E*), LP (*F*), or to LP/BafA (*H*).

(Fig. 3*C* and Supplementary Fig. 3*C*) and phosphorylation of Akt (Fig. 3*D* and Supplementary Fig. 3*D* and *E*) and S6 (Fig. 3*E* and Supplementary Fig. 3*D* and *F*) occurred much later, namely, after 14 h of high-palmitate culturing. In conclusion, high-palmitate induces a set of early changes starting within 1 h and a set of later changes occurring after 14 h (Fig. 3*F*). Hence, v-ATPase inhibition arises well before the emergence of insulin resistance, which is suggestive of v-ATPase inhibition as mediator of lipid-induced insulin resistance.

Direct Inhibition of v-ATPase Induces Insulin Resistance

Inhibition of v-ATPase in HL-1 cardiomyocytes was achieved genetically via silencing of subunit B2 (which also led to downregulation of subunit a2) and pharmacologically via long-term bafilomycin-A treatment (Supplementary Fig. 4*E*, quantified in Fig. 4*A* and *B*). Both treatments decreased v-ATPase function by >70% (bafilomycin-A–sensitive chloroquine accumulation) (Fig. 4*C* and Supplementary Fig. 4*B*). Subsequently, the effect of v-ATPase

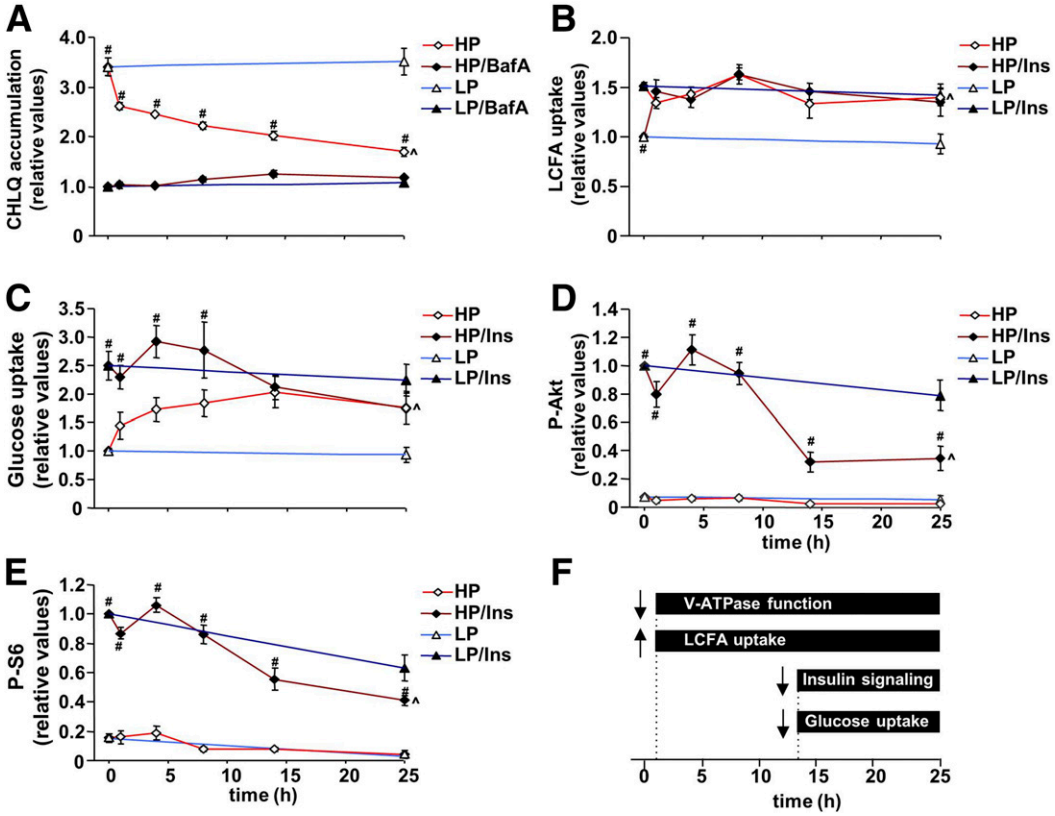

Figure 3—v-ATPase inhibition is an early event in lipid-induced insulin resistance. Rat cardiomyocytes were cultured with low palmitate (LP) or high palmitate (HP) for 0, 1, 3, 8, 15, and maximum to 25 h. *A*: Chloroquine (CHLQ) accumulation in cardiomyocytes treated without bafilomycin-A (BafA; LP and HP) and with 100 nmol/L BafA (LP/BafA and HP/BafA) for 15 min ($n = 6$). *B* and *E*: LCFA ($n = 4$–6) and glucose ($n = 6$) uptake and phosphorylation of Akt (P-Akt; $n = 6$) and S6 (P-S6; $n = 6$) in cardiomyocytes treated without insulin (LP and HP) and with 100 nmol/L insulin (LP/Ins and HP/Ins) for 15 min. Values are displayed as mean ± SEM. #Significance of HP vs. HP/BafA (*A*) and of HP/Ins vs. (*B–E*); $P < 0.05$. ^Significance of HP vs. LP (*A*) and of HP/Ins vs. LP/Ins (*B–E*); $P < 0.05$. Data were normalized to LP/$t = 0$ (*A–C*) or to LP/Ins/$t = 0$ (*D* and *E*). *F*: Overview of the data shown in panels *A–E* to highlight v-ATPase inhibition and lipid accumulation as early events before onset of insulin resistance. v-ATPase function is deduced from the degree of CHLQ accumulation and insulin signaling from the degree of Akt and S6 phosphorylation.

inhibition on insulin sensitivity was investigated in cells cultured with low palmitate concentrations that by themselves did not induce CD36 translocation or insulin resistance (Fig. 4*D–F* and Supplementary Fig. 4*C–G*: compare control [Ctrl] and low palmitate [LP]). Similar to high-palmitate culturing, genetic and pharmacological v-ATPase inhibition both caused a >1.6-fold increase in sarcolemmal CD36 content under basal conditions, which occurred at the cost of insulin-stimulated CD36 translocation (Fig. 4*D* and Supplementary Fig. 4*C*). Furthermore, v-ATPase inhibition (as well as high-palmitate treatment) caused a >40% decrease of insulin-stimulated Akt/S6 phosphorylation in HL-1 and primary cardiomyocytes (Fig. 4*E* and *F* and Supplementary Fig. 4*D–G* and *K–N*). Mitochondrial parameters and levels of reactive oxygen species were not altered (Supplementary Fig. 4*O–Q*). Ultimately, v-ATPase inhibition caused contractile dysfunction, as evident from the 64% decrease in sarcomere shortening (Fig. 4*G*). Yet, the contraction acceleration time and the duration of relaxation remained unaffected by bafilomycin-A (Fig. 4*H* and *I*). High-palmitate treatment also induced a decrease of sarcomere shortening of a similar magnitude without changes in contraction kinetics (Fig. 4*G–I*). Taken together, direct v-ATPase inhibition causes increased CD36 translocation to the sarcolemma, insulin resistance, and contractile dysfunction.

The Development of Insulin Resistance Induced by v-ATPase Inhibition Requires CD36

CD36 was silenced in HL-1 cardiomyocytes using siRNA (knockdown efficiency 50 ± 11% [$n = 3$]) (Supplementary Fig. 5*A* displays representative blot). As expected, CD36 silencing attenuated the development of the main features of high palmitate–induced insulin resistance, such as increased basal LCFA uptake and of losses of insulin-stimulated LCFA/glucose uptake and Akt/S6 phosphorylation (Fig. 5*A–D* and Supplementary Fig. 5*B–F*). In the low-palmitate condition, none of the parameters indicate the development of insulin resistance, whereas long-term bafilomycin-A treatment in this condition elicits changes similar to those found during high-palmitate culturing (Fig. 5*A–E*). Importantly, CD36 silencing fully prevented the bafilomycin-A–induced changes in LCFA uptake and insulin signaling (Fig. 5*A–D* and Supplementary Fig. 5*B–F*),

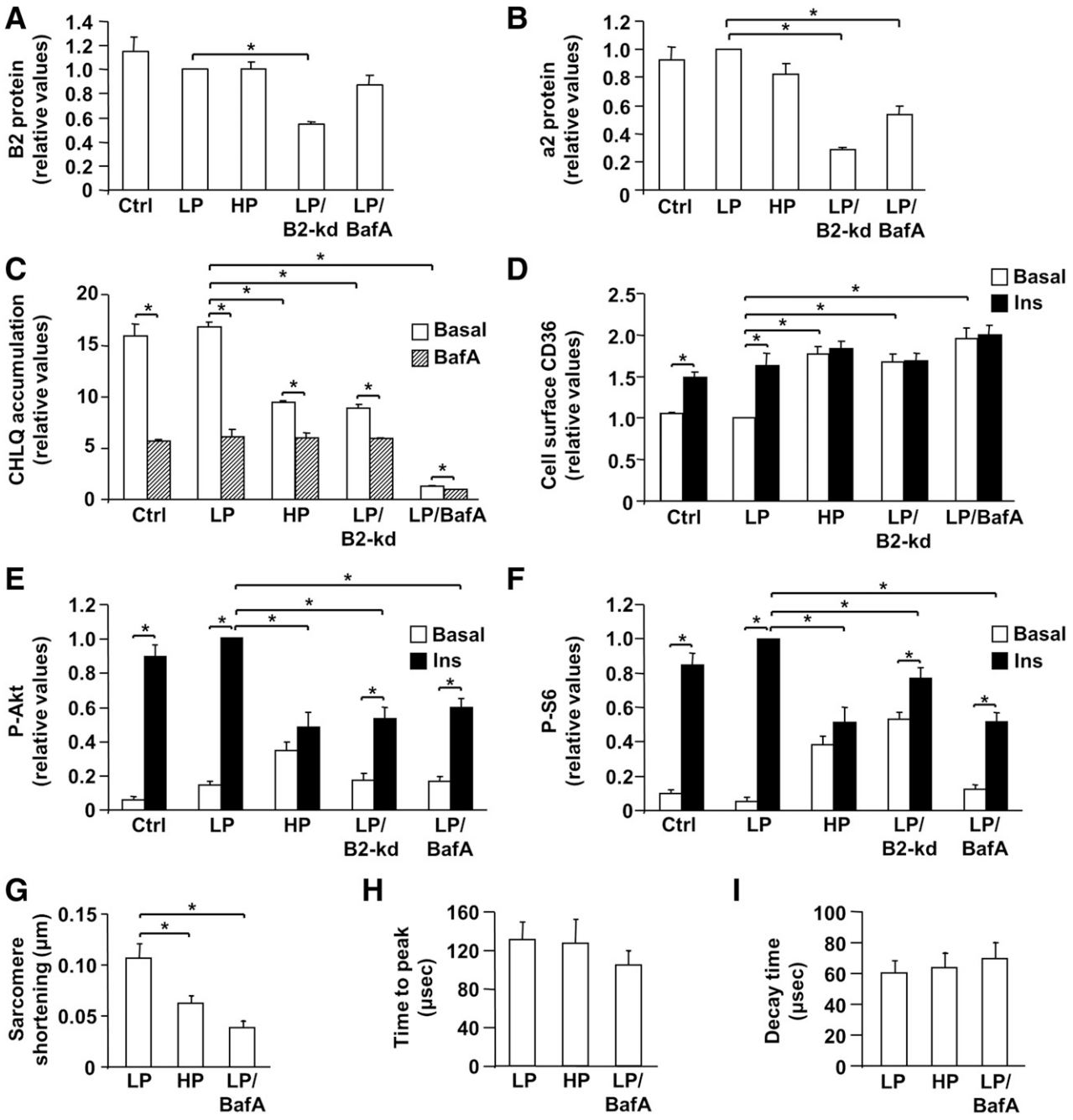

Figure 4—Direct inhibition of v-ATPase causes insulin resistance and contractile dysfunction in cardiomyocytes. *A–F*: HL-1 cardiomyocytes were transfected with negative control scrambled siRNA or with siRNA targeting v-ATPase B2 subunit mRNA (B2-kd). At 32 h after transfection, cells were cultured under control condition (Ctrl), or with low palmitate (LP), high palmitate (HP), or LP enriched with 100 nmol/L bafilomycin-A (LP/BafA) for 16 h. *A* and *B*: Protein expression of v-ATPase a2 ($n = 4$) and B2 subunits ($n = 6$). *C*: Chloroquine (CHLQ) accumulation in cardiomyocytes treated without (basal)/with 100 nmol/L BafA for 25 min ($n = 4$). *D–F*: Sarcolemmal (i.e., cell surface) CD36 content ($n = 6$) and phosphorylation of Akt (P-Akt, $n = 8$) and S6 (P-S6, $n = 4$) in cardiomyocytes treated without (basal)/with 100 nmol/L insulin (Ins) for 30 min. *G–I*: Rat cardiomyocytes were incubated in LP, HP, or LP/BafA for 25 h. Several parameters of contraction were determined upon 1 Hz electrostimulation: sarcomere shortening (*G*), the time from the onset of the contraction to its peak (time to peak) (*H*), and the time of decay of the contraction to 50% of its peak (decay time) ($n = 4$; imaging of 5 cells/condition) (*I*). Values are displayed as mean ± SEM. *$P < 0.05$. Data were normalized to LP (*A* and *B*), LP/BafA (*C*), LP/basal (*D*), or to LP/Ins (*E* and *F*).

therefore disclosing the requirement of CD36 for the development of insulin resistance resulting from v-ATPase inhibition. CD36 silencing also fully prevented the high palmitate–induced loss of chloroquine accumulation (Fig. 5*E* and Supplementary Fig. 5*G*), thus indicating that CD36-mediated LCFA uptake is responsible for v-ATPase inhibition. These findings were further confirmed in primary cardiomyocytes, in which an immunological CD36

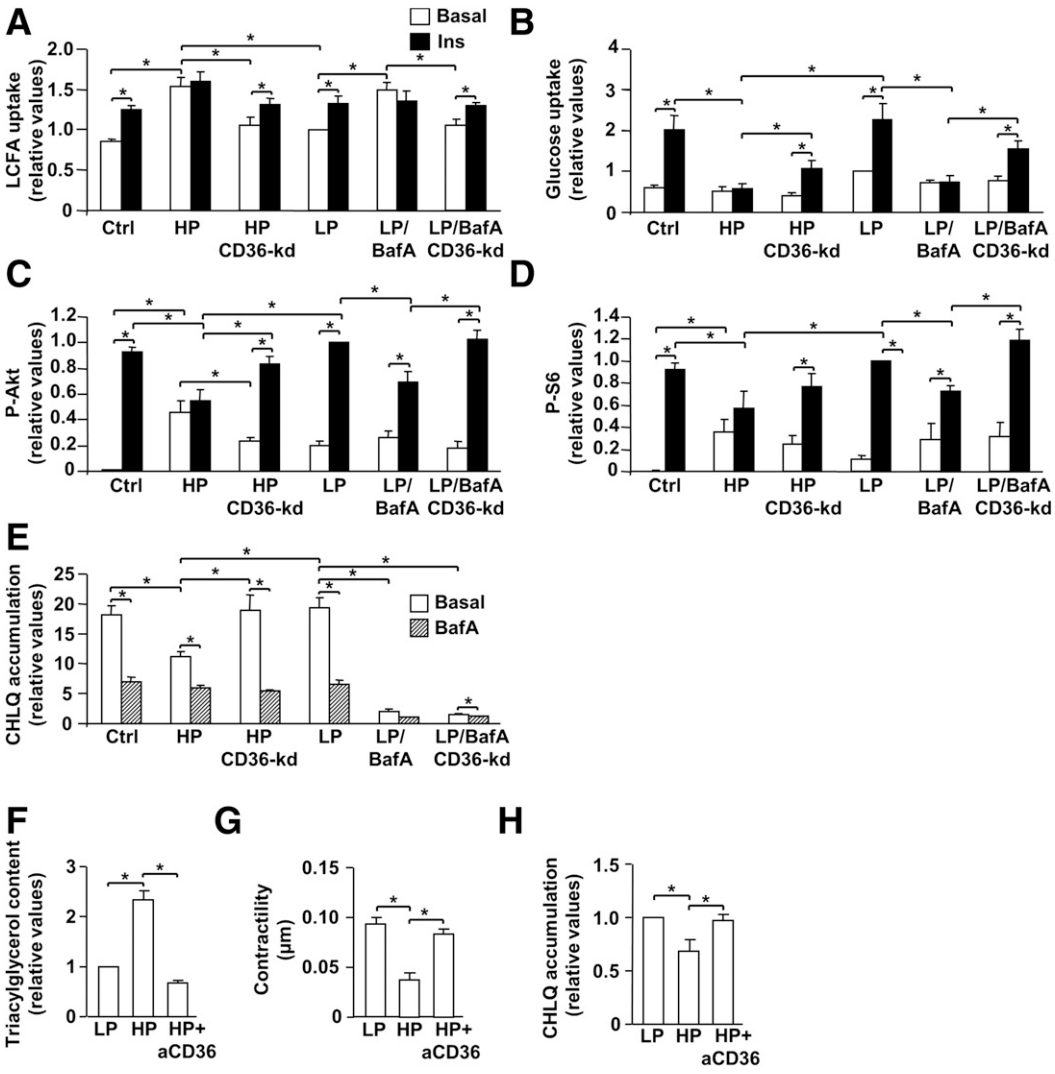

Figure 5—Direct v-ATPase inhibition requires CD36 to develop insulin resistance and contractile dysfunction. *A–E*: HL-1 cardiomyocytes (HL-1) were transfected with negative control scrambled siRNA or siRNA targeting CD36 mRNA (CD36-kd). At 32 h after transfection, cells were cultured under control condition (Ctrl), or with high palmitate (HP), low palmitate (LP), or LP enriched with 100 nmol/L bafilomycin-A (LP/BafA) for 16 h. *A–D*: LCFA (n = 5) and glucose (n = 5) uptake and phosphorylation of Akt (P-Akt; n = 6) and S6 (P-S6; n = 6) in HL-1 treated without (basal)/with 100 nmol/L insulin (Ins) for 30 min. *E*: Chloroquine (CHLQ) accumulation in HL-1 treated without (basal)/with 100 nmol/L BafA for 25 min (n = 6). *F–H*: Rat cardiomyocytes were incubated for 48 h with LP, HP, or HP with addition of 0.83 μg/mL anti–CD36 clone 63 (aCD36). *F*: Triacylglycerol content (n = 5). *G*: Sarcomere shortening upon 1 Hz electrostimulation (n = 5). *H*: CHLQ accumulation in cardiomyocytes treated without (basal)/with 100 nmol/L BafA (25 min) (n = 3). Values are displayed as mean ± SEM. *P < 0.05. Data were normalized to LP/basal (*A* and *B*), LP/Ins (*C* and *D*), LP/BafA (*E*), or to LP (*F* and *H*).

blockade via monoclonal antibody clone 63 prevented lipid accumulation and loss of contractility and v-ATPase function (Fig. 5*F–H*). We previously demonstrated that application of clone 63 preserved insulin sensitivity and contractile function in high palmitate–treated cardiomyocytes via inhibiting LCFA uptake (17). Thus, CD36-mediated LCFA uptake is required for v-ATPase inhibition and subsequent development of insulin resistance and contractile dysfunction.

Human Cardiomyocytes Display Reduced v-ATPase Function Upon Lipid Oversupply

Human iPSCs were differentiated into iPSC-CMs. Fourteen days after the cardiomyocyte differentiation protocol was initiated, >30% of the cells displayed spontaneous contractions, and the cardiospecific proteins myosin heavy chain (α-isoform; MYH6) and cardiac troponin T (TNNT2) were upregulated by 4.5- and 2.8-fold, respectively (Fig. 6*A*). Similar to rodent cardiomyocytes (Figs. 1–5), iPSC-CMs developed the main features of insulin resistance upon high-palmitate culturing: loss of insulin-stimulated LCFA/glucose uptake and increased basal LCFA uptake, as well as loss of insulin-stimulated Akt/S6 phosphorylation (Fig. 6*B–D* and Supplementary Fig. 6*A* and *B*). Moreover, iPSC-CMs cultured with high palmitate display loss of chloroquine accumulation (Fig. 6*E* and Supplementary Fig. 6*C*). Therefore, the mechanism of lipid-induced v-ATPase inhibition leading to insulin

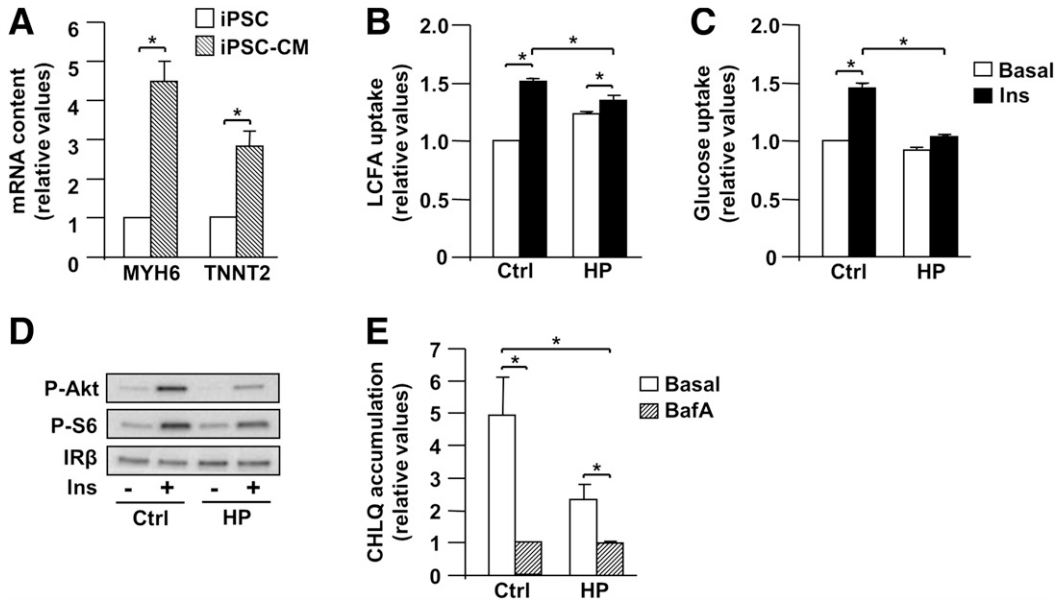

Figure 6—Inhibition of v-ATPase replicates in human iPSC-CMs upon lipid overload. Human iPSC-CMs were cultured for 16 h in control (Ctrl) or high-palmitate (HP) media. *A*: mRNA expression of MYH6 and TNNT2 in iPSC-CM vs. undifferentiated iPSC ($n = 3$). *B–D*: LCFA and glucose uptake ($n = 4$) and phosphorylation of Akt (P-Akt) and S6 (P-S6) ($n = 3$; representative blots are displayed) in human iPSC-CMs treated without (basal)/with 100 nmol/L insulin (Ins) for 30 min. Loading control: insulin receptor-β (IRβ). *E*: Chloroquine (CHLQ) accumulation in human iPSC-CM treated without (basal)/with 100 nmol/L bafilomycin-A (BafA) for 25 min. Values are displayed as mean ± SEM. $^*P < 0.05$. Data were normalized to iPSC (*A*), Ctrl/basal (*B* and *C*), or to Ctrl/BafA (*E*).

resistance appears conserved between species and thus applicable to the human heart.

Lipid-Induced v-ATPase Inhibition Is Caused by Disassembly of the V_0/V_1 Subcomplexes

In earlier studies in yeast, reversible disassembly of v-ATPase into its two subcomplexes, V_0 and V_1, was described as a main mechanism of regulation of this protein (13,15). Thus, HL-1 cardiomyocytes were cultured in high-palmitate and control media, subsequently lysed in the presence of mild detergents, and used for immunoprecipitation with antibodies against the a2 or B2 subunits of v-ATPase. To assess the degree of assembly, we exploited that a2 is part of the V_0 subcomplex and that B2 is part of the V_1 subcomplex. For both immunoprecipitations, we observed that the degree of coimmunoprecipitation with the other subunit under high-palmitate culturing conditions was markedly lower than under basal conditions (Fig. 7*A*), indicating V_0/V_1 disassembly.

We also applied subcellular fractionation to study the V_0/V_1 assembly status. HL-1 cardiomyocytes were fractionated into subcellular membranes and cytoplasm. The a2 subunit, as an indicator of the membrane-bound V_0 subcomplex, was found predominantly in the membrane fraction (Fig. 7*B*). As part of the soluble V_1 subcomplex, B2 markedly shifted from the membranous to the cytoplasmic fraction upon high-palmitate culturing versus the control condition (Fig. 7*B*). CD36 silencing prevented this shift of B2 from membranes to the cytoplasm (Fig. 7*B*). Together, these findings indicate that lipid overexposure inhibits v-ATPase by means of V_0/V_1 disassembly in a CD36-dependent manner.

Oleate Induces v-ATPase Inhibition but Does Not Produce Insulin Resistance

Whereas palmitate is the most abundant saturated LCFA in food, oleate is the predominant unsaturated LCFA. Oleate inhibited v-ATPase activity in a similar manner as palmitate (Fig. 8*A*). Yet, oleate induced triacylglycerol accumulation but not insulin resistance (Fig. 8*B* and *C*).

DISCUSSION

The obtained results led us to formulate the following conclusions: *1*) Upon palmitate overload in cardiomyocytes, v-ATPase activity decreases, leading to endosomal alkalinization and thereafter to the onset of insulin resistance and contractile dysfunction. *2*) Palmitate-induced v-ATPase inhibition involves V_0/V_1 disassembly and requires CD36-mediated lipid uptake. *3*) Oleate inhibits v-ATPase to increase its uptake and subsequent storage without causing insulin resistance. These aspects are further discussed below.

Lipid-Induced v-ATPase Inhibition Precedes the Onset of Insulin Resistance

Feeding rats a high-fat diet causes increased CD36 translocation to the sarcolemma and increased LCFA uptake, followed by lipid accumulation, impaired insulin signaling and insulin-stimulated glucose uptake, cardiac morphological changes, and, finally, contractile dysfunction (8). In the current study, the lipid-induced manifestations occurred in conjunction with v-ATPase inhibition in rodent and human cardiomyocytes upon lipid oversupply in vivo and in vitro (Figs. 1, 2, and 6). Importantly, v-ATPase inhibition is an

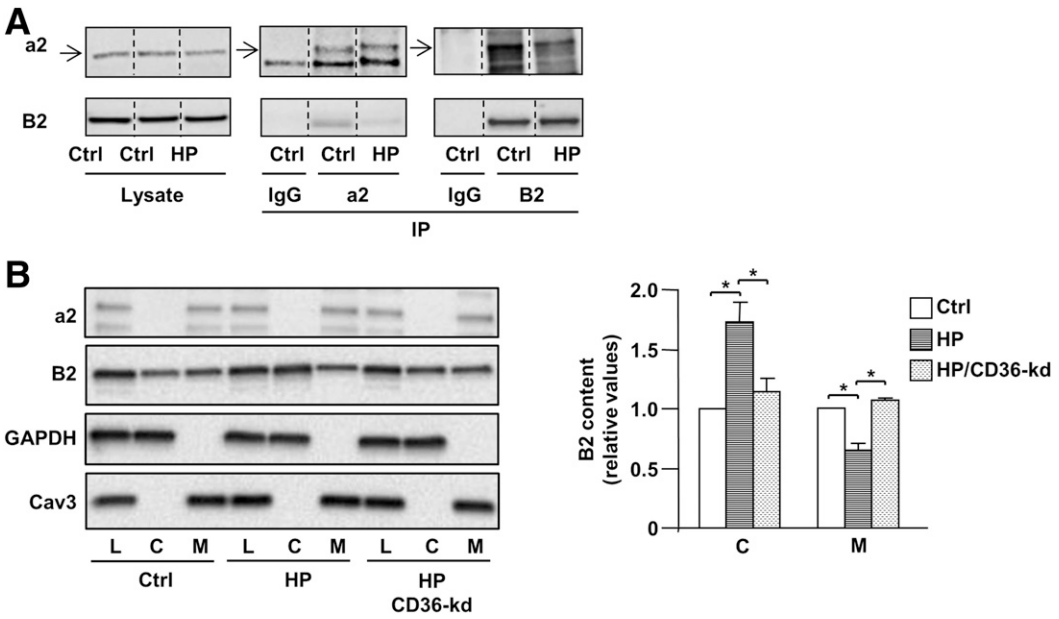

Figure 7—Lipids induce inhibition of v-ATPase via its disassembly into V_0 and V_1 subcomplexes. HL-1 cardiomyocytes were transfected with negative control scrambled siRNA or siRNA targeting CD36 mRNA (CD36-kd). At 32 h after transfection, cells were cultured for 16 h in control medium (Ctrl) or with high palmitate (HP) and subsequently used for immunoprecipitation (IP) (*A*) or fractionation (*B*). *A*: Content of v-ATPase subunits a2 and B2 in cell lysates (L) and in IPs using control IgG or antibodies capturing a2 and B2 (n = 3). The dotted lines between the lanes indicate that these lanes were not adjacent to each other in the original gel, but nonetheless, were derived from the same blots. *B*: Content of a2 and B2 in cytoplasmic fraction (C) and membrane fraction (M). GAPDH was the loading control for C, and caveolin-3 (Cav3) was the loading control for M (n = 3–7). B2 content of the cytoplasmic fraction was normalized against GAPDH and B2 content of the membrane fraction against Cav3. Immunoblots are representative results.

early event already occurring within 1 h after high-palmitate addition that is simultaneous with a 1.5-fold increase in myocellular LCFA uptake (Fig. 3 and Supplementary Fig. 3). This rapid increase in basal LCFA uptake upon the start of the high-palmitate treatment occurred at the cost of insulin-stimulated LCFA uptake, which was completely blunted (Fig. 3*B*). Furthermore, high palmitate–induced CD36 translocation renders the cells insensitive to further insulin-stimulated CD36 translocation (Fig. 4*D*). Hence, an insulin-responsive CD36-containing endosomal subcompartment might provide the source of CD36 for translocation in lipid-overexposed cells. Notably, the impairment of insulin signaling and insulin-stimulated glucose uptake followed much later (i.e., at 14 h after high-palmitate addition), indicating that v-ATPase inhibition and CD36 translocation precede the high palmitate–induced insulin resistance. These present results are furthermore in good agreement with our recent in vivo findings (22), where we observed rapid increases in CD36 translocation to the sarcolemma and in myocellular LCFA uptake, accumulation of triacylglycerol and diacylglycerol (2–3 days), and a delayed impairment in insulin signaling and GLUT4 translocation (>21 days). Therefore, the processes that underlie the progression from lipid accumulation into insulin resistance appear complex and more time consuming than the relatively fast occurring v-ATPase inhibition and consequent acceleration of CD36-mediated lipid uptake.

v-ATPase Inhibition Requires CD36 to Cause Insulin Resistance and Contractile Dysfunction

The early onset of v-ATPase inhibition in lipid-induced insulin resistance is suggestive of a causal involvement. Direct evidence for a causal role of v-ATPase in lipid-induced insulin resistance was obtained by *1*) siRNA-mediated silencing of v-ATPase and *2*) long-term bafilomycin-A treatment of cardiomyocytes in the presence of a low amount of extracellular palmitate. Both strategies markedly inhibited v-ATPase function, increased CD36 translocation to the sarcolemma, and caused insulin resistance in a similar manner as in high palmitate–treated cardiomyocytes. With respect to contractile activity, v-ATPase inhibition in cardiomyocytes caused a marked decrease in sarcomere shortening, which is of similar magnitude as seen upon high-palmitate treatment of cardiomyocytes. Moreover, no changes occurred in contraction acceleration or relaxation time, making it unlikely that v-ATPase inhibition negatively affects sarcomere shortening via a general toxic action mechanism. Such a general toxic effect would not only decrease the contraction amplitude but also increase the relaxation time, as seen, for example, by mitochondrial inhibition (23). Hence, our investigations causally link v-ATPase inhibition not only to lipid-induced insulin resistance but also to contractile dysfunction, thereby suggesting that endosomal alkalinization underlies the metabolic and functional alterations that are known characteristics of lipid-induced cardiomyopathy.

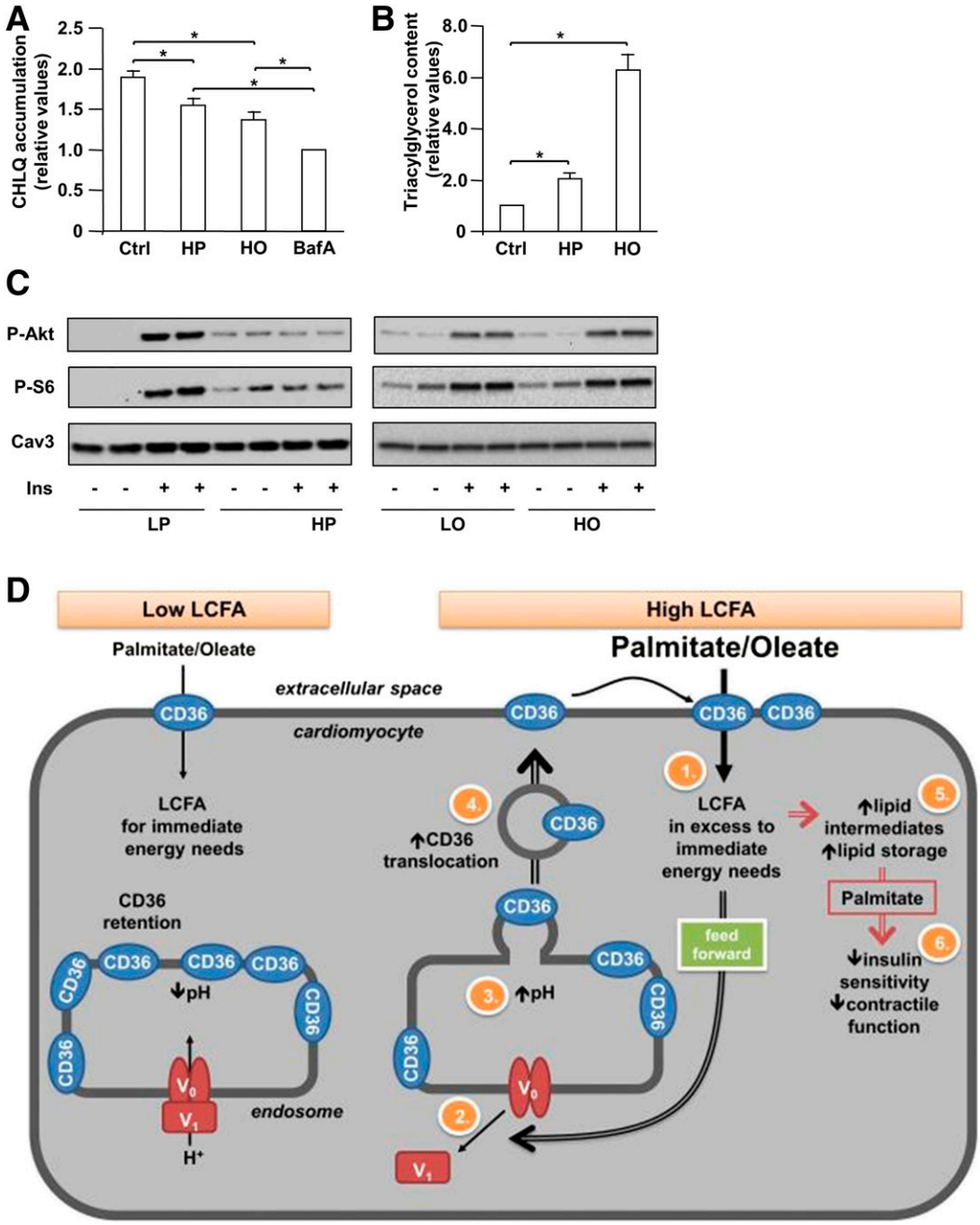

Figure 8—LCFA specificity and mechanism of lipid-induced v-ATPase inhibition. HL-1 cardiomyocytes (HL-1) were cultured under control condition (Ctrl), with high palmitate (HP) or high oleate (HO) for 16 h. *A*: Chloroquine (CHLQ) accumulation in HL-1 treated without/with 100 nmol/L bafilomycin-A (BafA) for 25 min ($n = 6$). *B*: Triacylglycerol content ($n = 6$). *C*: Phosphorylation of Akt (P-Akt; $n = 3$) and S6 (P-S6; $n = 3$) in cardiomyocytes treated without/with 100 nmol/L insulin (Ins) for 30 min. Cav3, caveolin-3; LO, low oleate; LP, low palmitate. Values are displayed as mean ± SEM. $^*P < 0.05$. *D*: Schematic presentation of lipid-induced v-ATPase inhibition shows the consequences for insulin sensitivity and contractile function. When the LCFA supply of oleate or palmitate is low, CD36 is primarily found in endosomes. Furthermore, the v-ATPase V_0 subcomplex, which is integral to the endosomal membrane, is assembled with the cytosolic V_1 subcomplex, allowing for acidification of the endosomal lumen. In this situation, the available LCFA is metabolized to meet the immediate energy demand. Elevated extracellular LCFA supply triggers a series of events: *1*) Increased CD36-mediated LCFA uptake results in elevated intramyocellular LCFA levels. *2*) LCFA causes the V_1 and V_0 subcomplexes to dissociate. *3*) Therefore, V_1 is shifted toward the cytoplasm. *4*) The disassembly of v-ATPase leads to endosomal alkalinization. Increased endosomal pH triggers the translocation of CD36 vesicles to the sarcolemma. Upon chronic lipid oversupply, where LCFA uptake surpasses the metabolic needs, further processes are set in motion. *5*) The lipid-induced increase in sarcolemmal CD36 feeds forward to further increased LCFA uptake and progressive lipid storage. *6*) Palmitate overload culminates into loss of insulin sensitivity and contractile function.

How is v-ATPase inhibited by lipid overexposure? We speculated on a causal role of CD36-mediated LCFA uptake. Indeed, CD36 downregulation prevented high palmitate–induced v-ATPase inhibition (Fig. 5*E* and *H*) (i.e., pointing to impairment of v-ATPase function as a consequence of CD36-mediated LCFA uptake). Moreover, CD36 downregulation prevented increased LCFA uptake (Fig. 5*B*), insulin resistance (Fig. 5*C* and *D*, and Supplementary Fig. 5*D–F*), and contractile dysfunction (Fig. 5*H*). Taken together, we describe a novel v-ATPase–CD36 interplay showing its critical involvement in the development of lipid-induced insulin resistance and contractile dysfunction.

Cycles of assembly/disassembly appeared to be the main mechanism of regulation of v-ATPase activity in yeast (13,15). Hence, we speculated that lipids cause v-ATPase disassembly into the two subcomplexes, V_0 (that remains integral within the endosomal membrane) and V_1 (that will drift away into the cytoplasm). Indeed, using two different methods (immunoprecipitation and subcellular fractionation), we demonstrated that lipids induce disassembly of v-ATPase and migration of V_1 into the cytoplasm (Fig. 7). Together, this indicates v-ATPase as a possible lipid sensor in cardiomyocytes.

Oleate Inhibits v-ATPase Function Without Causing Insulin Resistance

Oleate and palmitate alike inhibited v-ATPase activity. However, downstream of v-ATPase, oleate exerted different cellular actions than palmitate: oleate led to triacylglycerol accumulation but did not elicit insulin resistance, as also previously observed (24,25). What are the main differences between these LCFAs that could explain the observations? In particular, palmitate uptake may lead to ceramide accumulation (24), which has been linked to the development of insulin resistance (11). Conversely, oleate uptake may be coupled to storage within "inert" lipid droplets and/or could exert cardioprotective roles (26).

With respect to the mechanism of v-ATPase inhibition, which likely is similar for oleate and palmitate, we searched for a feasible answer to explain how lipids might cause v-ATPase disassembly. Interestingly, v-ATPase disassembly in neuronal cells appears to be induced by palmitoylation (27). Given that various proteins undergo palmitoylation and oleoylation at the same cysteine residue (28), the disassembly signal might include long-chain fatty acylation at a specific cysteine within one of the v-ATPase subunits. Further studies are warranted to clarify the exact regulation of v-ATPase assembly/disassembly by lipids in cardiomyocytes.

Proposed Model

We identify v-ATPase V_0/V_1 disassembly as a trigger of increased CD36 translocation and thus describe a novel function of v-ATPase. Further, CD36-mediated lipid uptake upon lipid supply feeds forward to increased CD36 translocation to the sarcolemma and further increased lipid uptake. Accordingly, chronic lipid oversupply by inhibiting v-ATPase gives rise to a vicious cycle of accelerated myocellular lipid accumulation, which, in the case of palmitate, sets the heart on a road to insulin resistance and contractile dysfunction (Fig. 8). Because the mechanism of lipid-induced v-ATPase inhibition is conserved in human cardiomyocytes, the identification of pharmacological agents that stabilize the assembly of v-ATPase V_1/V_0 subcomplexes may be considered as a possible novel strategy to combat cardiac lipid overload.

Acknowledgments. The authors thank Ilvy Geraets (Department of Molecular Genetics, Maastricht University) for her excellent technical assistance.

Funding. Y.L. received support from the Chinese Scholarship Council. M.N. and D.N. are recipients of Veni and Vidi Innovational Research Grants from the Netherlands Organization of Scientific Research (NWO-ZonMw grant no. 916.14.050 and NWO-ALW grant no. 864.10.007, respectively). D.C. is the recipient of a Marie Curie Fellowship (grant PIIF-GA-2012-332230).

Duality of Interest. No potential conflicts of interest relevant to this article were reported.

Author Contributions. Y.L., L.K.M.S., M.N., M.v.Z., G.A., D.N., and J.J.F.P.L. analyzed data. Y.L., L.K.M.S., D.K., P.S., W.A.C., A.G., and D.C. performed the experiments. Y.L., L.K.M.S., J.F.C.G., D.N., and J.J.F.P.L. designed the experiments. Y.L., D.N., and J.J.F.P.L. wrote the manuscript. P.J.S. generated clone 63. All authors discussed the data and commented on the manuscript before submission. J.J.F.P.L. is the guarantor of this work and, as such, had full access to all the data in the study and takes responsibility for the integrity of the data and the accuracy of the data analysis.

Prior Presentation. Parts of this study were an oral presentation at the 76th Scientific Sessions of the American Diabetes Association, New Orleans, LA, 10–14 June 2016.

References

1. Szczepaniak LS, Victor RG, Orci L, Unger RH. Forgotten but not gone: the rediscovery of fatty heart, the most common unrecognized disease in America. Circ Res 2007;101:759–767

2. Harmancey R, Taegtmeyer H. The complexities of diabetic cardiomyopathy: lessons from patients and animal models. Curr Diab Rep 2008;8:243–248

3. Glatz JF, Luiken JJ, Bonen A. Membrane fatty acid transporters as regulators of lipid metabolism: implications for metabolic disease. Physiol Rev 2010;90:367–417

4. Wilson CR, Tran MK, Salazar KL, Young ME, Taegtmeyer H. Western diet, but not high fat diet, causes derangements of fatty acid metabolism and contractile dysfunction in the heart of Wistar rats. Biochem J 2007;406:457–467

5. Sverdlov AL, Elezaby A, Behring JB, et al. High fat, high sucrose diet causes cardiac mitochondrial dysfunction due in part to oxidative post-translational modification of mitochondrial complex II. J Mol Cell Cardiol 2015;78:165–173

6. Luiken JJ, Koonen DP, Willems J, et al. Insulin stimulates long-chain fatty acid utilization by rat cardiac myocytes through cellular redistribution of FAT/CD36. Diabetes 2002;51:3113–3119

7. Coort SL, Hasselbaink DM, Koonen DP, et al. Enhanced sarcolemmal FAT/CD36 content and triacylglycerol storage in cardiac myocytes from obese Zucker rats. Diabetes 2004;53:1655–1663

8. Ouwens DM, Diamant M, Fodor M, et al. Cardiac contractile dysfunction in insulin-resistant rats fed a high-fat diet is associated with elevated CD36-mediated fatty acid uptake and esterification. Diabetologia 2007;50:1938–1948

9. Yang J, Sambandam N, Han X, et al. CD36 deficiency rescues lipotoxic cardiomyopathy. Circ Res 2007;100:1208–1217

10. Steinbusch LK, Luiken JJ, Vlasblom R, et al. Absence of fatty acid transporter CD36 protects against Western-type diet-related cardiac dysfunction following pressure overload in mice. Am J Physiol Endocrinol Metab 2011;301:E618–E627

11. Savage DB, Petersen KF, Shulman GI. Disordered lipid metabolism and the pathogenesis of insulin resistance. Physiol Rev 2007;87:507–520
12. Steinbusch LK, Wijnen W, Schwenk RW, et al. Differential regulation of cardiac glucose and fatty acid uptake by endosomal pH and actin filaments. Am J Physiol Cell Physiol 2010;298:C1549–C1559
13. Bond S, Forgac M. The Ras/cAMP/protein kinase A pathway regulates glucose-dependent assembly of the vacuolar (H+)-ATPase in yeast. J Biol Chem 2008;283:36513–36521
14. Ma B, Xiang Y, An L. Structural bases of physiological functions and roles of the vacuolar H(+)-ATPase. Cell Signal 2011;23:1244–1256
15. Kane PM. Targeting reversible disassembly as a mechanism of controlling V-ATPase activity. Curr Protein Pept Sci 2012;13:117–123
16. Luiken JJ, van Nieuwenhoven FA, America G, van der Vusse GJ, Glatz JF. Uptake and metabolism of palmitate by isolated cardiac myocytes from adult rats: involvement of sarcolemmal proteins. J Lipid Res 1997;38:745–758
17. Angin Y, Steinbusch LK, Simons PJ, et al. CD36 inhibition prevents lipid accumulation and contractile dysfunction in rat cardiomyocytes. Biochem J 2012; 448:43–53
18. Schwenk RW, Dirkx E, Coumans WA, et al. Requirement for distinct vesicle-associated membrane proteins in insulin- and AMP-activated protein kinase (AMPK)-induced translocation of GLUT4 and CD36 in cultured cardiomyocytes. Diabetologia 2010;53:2209–2219
19. Schwenk RW, Angin Y, Steinbusch LK, et al. Overexpression of vesicle-associated membrane protein (VAMP) 3, but not VAMP2, protects glucose transporter (GLUT) 4 protein translocation in an in vitro model of cardiac insulin resistance. J Biol Chem 2012;287:37530–37539
20. Luiken JJ, Vertommen D, Coort SL, et al. Identification of protein kinase D as a novel contraction-activated kinase linked to GLUT4-mediated glucose uptake, independent of AMPK. Cell Signal 2008;20:543–556
21. Luiken JJ, Aerts JM, Meijer AJ. The role of the intralysosomal pH in the control of autophagic proteolytic flux in rat hepatocytes. Eur J Biochem 1996;235:564–573
22. Bonen A, Jain SS, Snook LA, et al. Extremely rapid increase in fatty acid transport and intramyocellular lipid accumulation but markedly delayed insulin resistance after high fat feeding in rats. Diabetologia 2015;58:2381–2391
23. Kettlewell S, Cabrero P, Nicklin SA, Dow JA, Davies S, Smith GL. Changes of intra-mitochondrial Ca2+ in adult ventricular cardiomyocytes examined using a novel fluorescent Ca2+ indicator targeted to mitochondria. J Mol Cell Cardiol 2009;46:891–901
24. Listenberger LL, Han X, Lewis SE, et al. Triglyceride accumulation protects against fatty acid-induced lipotoxicity. Proc Natl Acad Sci U S A 2003;100:3077–3082
25. Gillet C, Spruyt D, Rigutto S, et al. Oleate abrogates palmitate-induced lipotoxicity and proinflammatory response in human bone marrow-derived mesenchymal stem cells and osteoblastic cells. Endocrinology 2015;156:4081–4093
26. Perdomo L, Beneit N, Otero YF, et al. Protective role of oleic acid against cardiovascular insulin resistance and in the early and late cellular atherosclerotic process. Cardiovasc Diabetol 2015;14:75
27. Bagh M, Chandra, G, Peng S, Zhang Z, Mukherjee A. A lysosomal targeting defect of V0a1 suppresses V-ATPase activity elevating lysosomal pH in Ppt1-/- mice: amelioration by NtBuHA. FASEB J 2015;29(Suppl. 1):570.6
28. Montigny C, Decottignies P, Le Maréchal P, et al. S-palmitoylation and s-oleoylation of rabbit and pig sarcolipin. J Biol Chem 2014;289:33850–33861